www.sciencemag.org/cgi/content/full/319/5867/1232/DC1

Supporting Online Material for

Deeply Inverted Electron-Hole Recombination in a Luminescent Antibody-Stilbene Complex

Erik W. Debler, Gunnar F. Kaufmann, Michael M. Meijler, Andreas Heine, Jenny M. Mee, Goran Pljevaljčić, Angel J. Di Bilio, Peter G. Schultz, David P. Millar, Kim D. Janda, Ian A. Wilson, Harry B. Gray,* Richard A. Lerner*

*To whom correspondence should be addressed. E-mail: rlerner@scripps.edu (R.A.L.); hbgray@caltech.edu (H.B.G.)

Published 29 February 2008, *Science* **318**, 1232 (2008)
DOI: 10.1126/science.1153445

This PDF file includes:

Materials and Methods
Figs. S1 to S3
Tables S1 and S2
References

Other Supporting Online Material for this manuscript includes the following:
(available at www.sciencemag.org/cgi/content/full/319/5867/1232/DC1)

Movie S1

Material and Methods

Generation of scFv EP2-19G2 mutants and protein purification

The mutant scFv gene fragments were generated using standard site-directed mutagenesis PCR protocols using the wild-type EP2-19G2 scFv gene as template. The obtained scFv genes were subcloned into pET-Flag (derived from pET-15b, Novagen) and transformed into Escherichia coli BL21(DE3). Expression was induced with 0.5 mM isopropyl β-D-thiogalactoside, and FLAG-tagged scFv fragments were purified on anti-Flag mAb M2 affinity agarose (Sigma).

Steady-state spectral measurements

Absorption spectra were measured on a HP 8453 spectrometer in PBS (10 mM sodium phosphate, 150 mM NaCl, pH 7.4), 3% DMF cosolvent, at 21 °C. The dissolved oxygen was not purged. For all the absorption measurements, the concentration of hapten **1** was kept at 10 μM in the presence of excess antibody combining sites. The absorption spectra of the EP2-19G2 scFv solutions were used as background for correcting the spectra of the corresponding antibody-hapten complex solutions. Fluorescence spectra were measured on FluoroMax-2 fluorimeter. In a typical experiment, the slits were at 1 mm/1 mm, the excitation wavelength was 327 nm, and the spectrum was recorded from 350 to 600 nm with an increment of 0.5 nm. The integration time was 1 s and the number of iterations was 10. The concentration of **1** was kept at 15 nM and the scFv concentrations were kept at around 10 μM. Fluorescence spectra of antibody solutions were used as background to correct the fluorescence spectra of corresponding antibody-hapten complexes. The fluorescence anisotropies were measured on a PC1 Photon Counting Spectrofluorometer from ISS at slit sizes of 1 mm/1 mm. Quantum yields were measured by following the instruction at:

http://www.jobinyvon.com/usadivisions/Fluorescence/applications/quantumyieldstrad.pdf. The standard for the fluorescence quantum yield determinations of the different scFv-**1** complexes was quinine bisulfate in 0.5 N H_2SO_4 (Φ_f =0.546). With the excitation wavelength at 327 nm, the fluorescence spectra of different scFv-**1** complexes were recorded at the following concentrations: 10 nM, 20 nM, 30 nM, 40 nM and 50 nM with integration time 1 s and increment of 0.5 nm. The slits were set at 2 mm/3 mm. The fluorescence spectra of quinine bisulfate were recorded at concentrations: 10 nM, 20 nM, 30 nM, 40 nM, and 50 nM. The fluorescence spectra of the EP2-19G2-**1** complexes were recorded at antibody concentrations of 2 μM and EP2 concentrations of 5, 10, 15, and 20 nM with integration time 1 s and increment of 2 nm. The slits were set at 2 mm/3 mm. The K_d values were measured by fluorescence titration. 100, 200, 300, 400, 500, 600, 700, 1000, 2000, 3000, 4750 nM of the Fab and the scFv fragments were titrated against 150 nM and 500 nM of **1** for the Fab and the scFv's, respectively. The K_d was obtained from curve fitting to the one-site binding (hyperbola) equation $F = (F_{max} * [scFv]) / (K_d + [scFv])$ with the program GraphPad Prism 5, where F is the measured fluorescence at concentration [scFv]. A representative titration curve of the wild-type scFv is shown in Fig. S3.

Time-resolved spectroscopy

All time-resolved measurements were made using the time-correlated single-photon counting method (S*1*). Antibody complexes were prepared using 75 μM of scFv's and 3 μM of **1** in PBS (10 mM sodium phosphate, 150 mM NaCl, pH 7.4), with 3% DMF cosolvent. Measurements were obtained by using repetitive excitation by a pulsed laser (frequency-tripled output of a Coherent Mira Titanium-Sapphire laser, ca. 2 ps pulse width, and repetition rate of 3.8 MHz at 303 nm). Fluorescence emission was measured at right angles to the excitation beam and by using a polarizer set at the magic angle (54.7 relative to vertical). Emission was detected at 410

nm by using a microchannel plate photomultiplier (Hamamatsu R3809U-01) and standard time-correlated, single-photon counting electronics. Emission decays were recorded in 4096 channels with a time increment of 22 ps, and were normalized relative to the number of counts recorded in the peak channel (approximately 50,000). The instrument response function was recorded using scattered light (303 nm) from a dilute suspension of nondairy coffee creamer. Emission decays were fit using non-linear least squares regression following convolution of the fitting function with the instrument response function. A sum of one or more exponentials was used for the fitting function and the goodness of fit was determined by examination of χ^2 and of the weighted residuals. The intensity decays of the antibody-**1** complexes measured at each wavelength could only be satisfactorily fit by multi-exponential decays: $I(t) = S \Sigma_i \alpha_i \exp(-t/\tau_i)$, convoluted with the instrument response function, where S, α_i, and τ_i are the overall scaling factor, decay amplitude, and decay time of component i (Table S1).

Crystallography

Fab EP2-25C10 was produced by papain digest as previously described (S*2*). Crystallization experiments were performed by the sitting drop vapor diffusion method at 22.5°C. The Fab, concentrated to 15mg/ml in 50 mM acetate buffer pH 5.5, was crystallized in presence of 2-fold molar excess of stilbene derivative **1** from 1.5M $(NH_4)_2SO_4$, 0.2M Li_2SO_4, 0.1M Tris pH 7.0. For data collection, the crystal was flash-cooled to 100K using 25% glycerol as a cryoprotectant. Data were collected at the ALS synchrotron/ Berkeley on beamline 5.0.1 and processed and scaled with HKL2000 (Table S2) (S*3*). The structure of EP2-25C10 was determined by molecular replacement using the program Phaser (S*4*) and the coordinates of antibody HyHel 10 (PDB ID code 3HFM). The model was refined by alternating cycles of model building with the program O (S*5*) and refinement with Refmac5 (S*6*). During refinement, non-crystallographic

symmetry restraints were applied to all main-chain atoms in the two Fab molecules in the asymmetric unit, except for some loop regions. The final statistics are shown in Table S2. The quality of the structure was analyzed using the programs MolProbity (S*7*), WHAT IF (S*8*), and PROCHECK (S*9*). Figures 2 and 4 were prepared with PyMol (S*10*), and Figure 3 was prepared using Bobscript (S*11*). The coordinates and the structure factors are deposited at the PDB under accession code 2NZR.

Supporting Figures

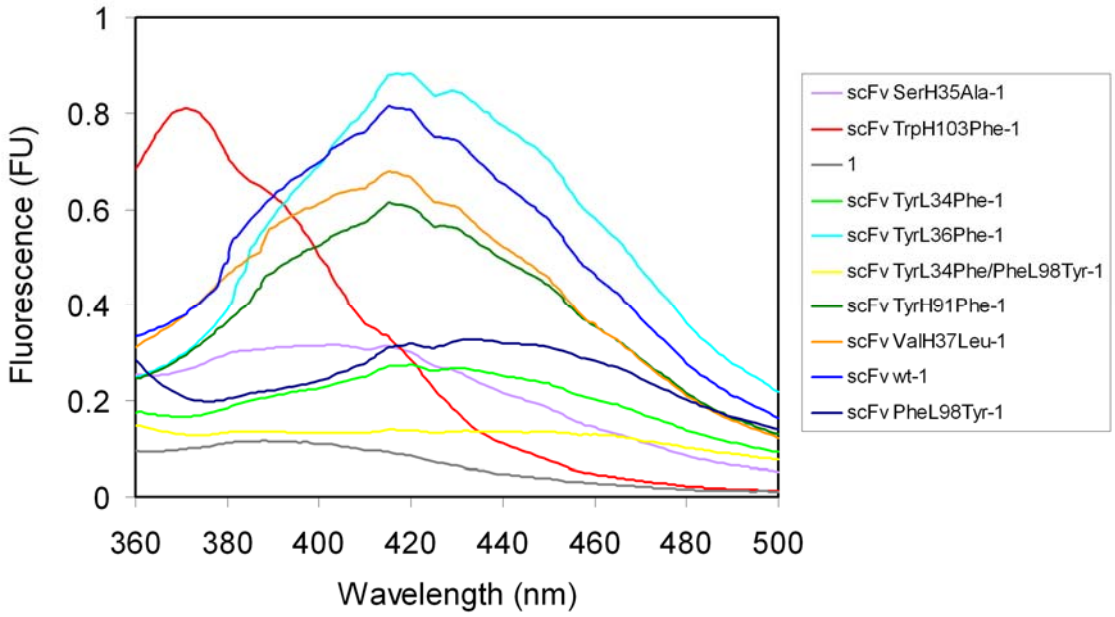

Figure S1. Fluorescence spectra of scFv mutants in complex with **1**, recorded in PBS buffer at room temperature. Excitation was at 327 nm. Note that the discrepancy in the intensities of some samples (e.g. scFv $Trp^{H103}Phe$) with respect to Fig. 1B is caused by varying protein concentrations of the scFv proteins during this initial screening.

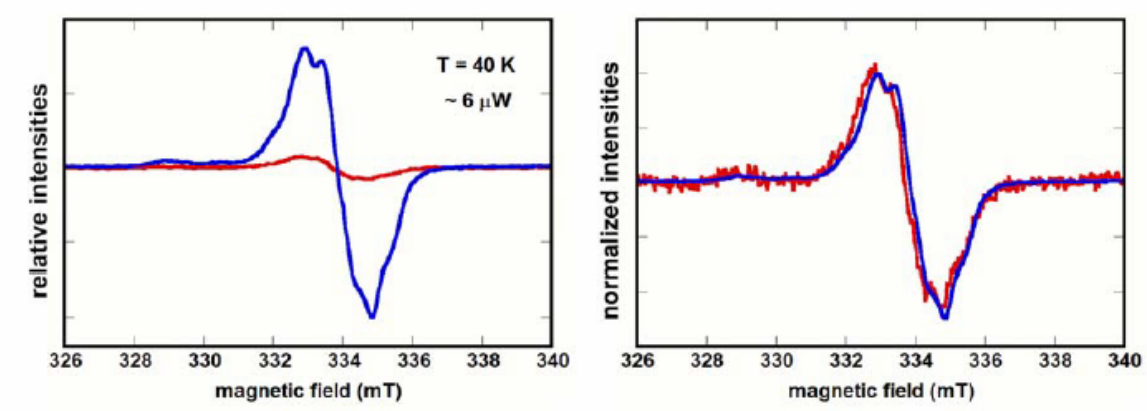

Figure S2. EPR spectrum of a sample containing ~100 µM EP2-19G2-**1** and excess $[Co(NH_3)_5Cl]^{2+}$ (KP_i, 40 K, 6 µW, mod. amplitude 1 G) measured after photolyis/freezing (blue

trace), and EPR spectrum of a similar sample that did not contain Co(III) quencher (red trace). The hyperfine structure bears the typical signature of a tyrosyl radical that may be generated by the oxidized Trp^{H103} of the charge-transfer complex in the excited state. Note that the lineshapes in absence and presence of Co(III) match (right panel), thereby suggesting that a tyrosyl radical is formed in both cases.

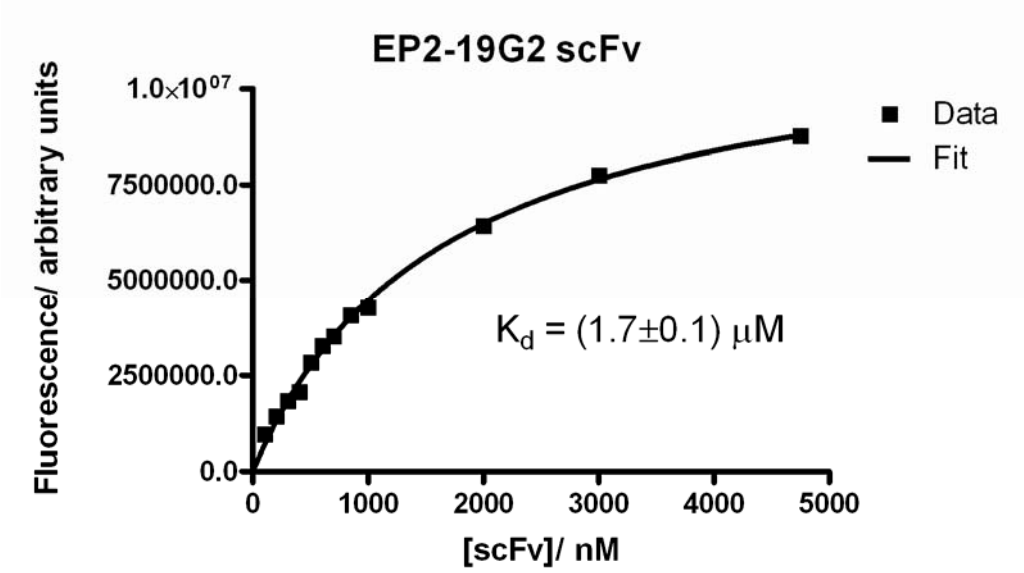

Figure S3. Fluorescence titration of the wild-type scFv of EP2-19G2 with **1** for K_d determination.

Supporting Tables

Table S1. Time-resolved fluorescence data of **1** and EP2-19G2-**1** complexes.

	α_1	τ_1 (ns)	α_2	τ_2 (ns)	α_3	τ_3 (ns)	α_4	τ_4 (ps)
1	1	0.0502						
Fab-**1**	0.331	22.8	0.0648	6.4	0.0988	0.762	0.506	24.5
scFv wt-**1**	0.170	22.7	0.0356	6.1	0.0743	0.754	0.720	45.1
scFv Trp^{H103}Phe-**1**	0.0009	15.6	0.5867	1.381	0.412	52.4		
scFv Tyr^{L34}Phe-**1**	0.022	34.5	0.0075	4.1	0.0382	0.772	0.932	50.5
scFv Tyr^{L36}Phe-**1**	0.273	30.3	0.0392	6.3	0.0848	0.882	0.603	46.2

Table S2. Data collection and refinement statistics of Fab EP2-25C10-**1**.

	Fab EP2-25C10-**1**
Space group	P1
Unit cell dimensions (Å)	a=60.0, b=72.5, c=77.2 α=92.0º, β=106.1º, γ=114.2º
Resolution range (Å)	30.0-2.50 (2.56-2.50) *
Unique reflections	37,156
Completeness (%)	97.9 (97.4)
Redundancy	1.9 (1.9)
R_{sym} †	0.08 (0.53)
$\langle I/\sigma \rangle$	11.1 (1.6)
R_{cryst} ‡/ R_{free} ‡	0.212/0.243
Fabs in asymmetric unit	2
Rmsd ¶ from ideal bond lengths (Å)/ angles (º)	0.013/ 1.3
Average B-values protein/ water/ stilbene ($Å^2$)	40.2/ 30.9/ 34.8
Ramachandran plot most favored/ additionally allowed/ generously allowed/ disallowed ‖ (%)	89.7/9.2/0.3/0.8

* Highest resolution shell.

† $R_{sym} = 100 \times \Sigma_{hkl} \Sigma_i | | F_i(hkl) | - | \langle F_i(hkl) \rangle | | / \Sigma_h \Sigma_i | F_i(hkl) |$

‡ $R_{cryst} = 100 \times \Sigma_{hkl} \, | \, |F_c(hkl)| - |F_o(hkl)| \, | \, / \, \Sigma_{hkl} \, | \, F_o(hkl) \, |$

§ R_{free} is calculated as for R_{cryst}, but from 5% of the data that was not used for refinement.

¶ Root-mean-square deviation.

‖ Thr^{L51}, Tyr^{H33}, and Asn^{H99} of both Fab EP2-25C10 molecules are the only residues in the disallowed region, but they all have well-defined electron density. Thr^{L51} is in a well-defined γ-turn, as in almost all other antibodies (S*12*).

References

S1. D.V. O'Connor, D. Phillips, *Time-Correlated Single Photon Counting* (Academic Press, London, 1984).
S2. E. Harlow, Lane, D, *Antibodies: A Laboratory Manual* (Cold Spring Harbor Laboratory, Cold Spring Harbor, N.Y., 1988)
S3. Z. Otwinowski, W. Minor, *Methods Enzymol.* **276**, 307 (1997).
S4. L. C. Storoni, A. J. McCoy, R. J. Read, *Acta Crystallogr. D* **60**, 432 (2004).
S5. T. A. Jones, J. Y. Zou, S. W. Cowan, M. Kjeldgaard, *Acta Crystallogr. A* **47**, 110 (1991).
S6. G. N. Murshudov, A. A. Vagin, E. J. Dodson, *Acta Crystallogr. D* **53**, 240 (1997).
S7. S. C. Lovell *et al.*, *Proteins* **50**, 437 (2003).
S8. G. Vriend, *J. Mol. Graph.* **8**, 52 (1990).
S9. R. A. Laskowski, M. W. MacArthur, D. S. Moss, J. M. Thornton, *J. Appl. Crystallogr.* **26**, 283 (1993).
S10. W. L. DeLano, *The PyMOL Molecular Graphics System* (DeLano Scientific, San Carlos, CA, USA, 2002)
S11. R. M. Esnouf, *Acta Crystallogr.* **D55**, 938 (1997).
S12. B. Al-Lazikani, A. M. Lesk, C. Chothia, *J. Mol. Biol.* **273**, 927 (1997).

Online Movie

Movie S1. Addition of antibody EP2-19G2 to a solution of the stilbene hapten **1** under UV illumination illustrates the striking difference between the faint purple fluorescence of **1** in absence of antibody and the intense powder-blue luminescence of the antibody-stilbene complex.